



Redistribution of Nickel Ions Embedded within Indium Phosphide Via Low Energy Dual Ion Implantations

Daniel C. Jones¹, Joshua M. Young¹, Wickramaarachchige J. Lakshantha¹, Satyabrata Singh¹, Todd A. Byers¹, Duncan L. Weathers¹, Floyd D. McDaniel^{1*}, Bibhudutta Rout¹

¹*Ion Beam Modification and Analysis Laboratory, Department of Physics, University of North Texas, Denton, Texas 76203, USA*

*Email: mcdaniel@unt.edu, bibhu@unt.edu

ARTICLE INFORMATION

Received: June 14
Revised: July 20, 2018
Accepted: July 24, 2018

Published online: August 6, 2018

Keywords:

InP based optoelectronics devices, Ni nanoclusters, Dual Ion Implantations, Rutherford Backscattering, X-ray Photoelectron Spectroscopy

DOI: [10.15415/jnp.2018.61002](https://doi.org/10.15415/jnp.2018.61002)

ABSTRACT

Transition-metal doped Indium Phosphide (InP) has been studied over several decades for utilization in optoelectronics applications. Recently, interesting magnetic properties have been reported for metal clusters formed at different depths surrounded by a high quality InP lattice. In this work, we have reported accumulation of Ni atoms at various depths in InP via implantation of Ni⁻ followed by H⁻ and subsequently thermal annealing. Prior to the ion implantations, the ion implant depth profile was simulated using an ion-solid interaction code SDTrimSP, incorporating dynamic changes in the target matrix during ion implantation. Initially, 50 keV Ni⁻ ions are implanted with a fluence of 2×10^{15} atoms cm⁻², with a simulated peak deposition profile approximately 42 nm from the surface. 50 keV H⁻ ions are then implanted with a fluence of 1.5×10^{16} atoms cm⁻². The simulation result indicates that the H⁻ creates damages with a peak defect center ~400 nm below the sample surface. The sample has been annealed at 450°C in an Ar rich environment for approximately 1hr. During the annealing, H vacates the lattice, and the formed nano-cavities act as trapping sites and a gettering effect for Ni diffusion into the substrate. The distribution of Ni atoms in InP samples are estimated by utilizing Rutherford Backscattering Spectrometry and X-ray Photoelectron Spectroscopy based depth profiling while sputtering the sample with Ar-ion beams. In the sample annealed after H implantation, the Ni was found to migrate to deeper depths of 125 nm than the initial end of range of 70 nm.

1. Introduction

Diluted magnetic semiconductors (DMS), especially III-V semiconductors, have become a major field of research over the last few decades. As Si based technology has begun to approach its limit in production viability, size, and power, DMS materials have been receiving increasing attention as a possible alternative. InP based materials do not face the present issues found in Si based integrated circuits (ICs). Si ICs need low defect densities to control the carrier lifetimes and decrease the junction leakage current [1]. Whereas in DMS, the defect densities could be used to control the circuit current and can be utilized to enhance ferromagnetic properties at the same time [2]. Presently in the DMS materials, the ferromagnetic properties can only be observed below room temperature [2]. To utilize these materials practically, ferromagnetism must be exhibited with a Curie temperature (T_c), at or above the room temperature [3]. The DMS materials can be synthesized using several approaches ranging from epitaxial growth to ion implantation, all of which rely on producing a specific

concentration of magnetic ions. To synthesize the DMS materials with existing methods, a 5% atomic concentration of transition metal dopant must be obtained [2]. This amount of doping causes numerous defects. These defects in the substrate lattice as well as the magnetic ions which have been incorporated into the lattice generate observable magnetic fields. These defects are believed to mediate the desired magnetic characteristics through the delocalization of hole concentration near the magnetic ion sites [3]. It is generally observed that annealing the samples at higher temperatures result in an increase of transition metal migration to cation lattice sites and hole density.

A potential solution in synthesizing DMS materials which can exhibit ferromagnetic behavior at room temperature, is the creation of small metal precipitates within a semiconductor that independently exhibit magnetic functionality, rather than relying on defects proportional to the hole concentrations. These small metal precipitates become magnetic nanoclusters. They can be conceptualized as a bulk ferromagnetic material with a net magnetization and measurable hysteresis loop as a function of applied

magnetic field for temperatures below T_c [4]. It has been theorized that synthesizing these magnetic nanoclusters in a high-quality crystal lattice will increase both their magnetic anisotropy and volume. These nanoclusters have been offered as an alternative to spin injection and collection in the semiconductor [5]. Irradiation with heavy ion beams along with post-thermal annealing has been an attractive technique for synthesis of metal clusters in semiconductors [6]. A major concern in this type of synthesis, is the ion induced damage in the substrate. The implanted region may be so heavily damaged by defects caused by the transition metals, that post implantation annealing may not fully restore a high quality crystal structure within the lattice [5]. This unfortunate defect mechanism associated with the implantation process can be overcome by a second ion implantation utilizing a light ion, such as H, subsequent to the initial implantation with a transition metal and high temperature annealing. This process can form nanoclusters and keep a high quality crystal phase in the semiconductor. The H implantation induces nano-cavities upon post implantation annealing to act as trapping sites for the transition metals by the dangling bonds left from the vacated H [7, 5, 8]. This work looks into using this novel technique to investigate re-distribution of Ni atoms at various depths beyond the initial heavy ion implant depth in the InP lattice. InP was specifically chosen for this research to look into the advancement of high power and frequency devices due to the high electron mobility inherent in this type of semiconductor.

2. Experimental

Prior to the ion implantation, the implant depth profiles were simulated using an ion-solid interaction code SDTrimSP (version 5.07) [9]. Commercially available high quality crystalline InP (100) samples were mounted on a sample stage in the low energy ion implantation line associated with a 9SDH-2 tandem accelerator (NEC, USA) at the Ion Beam Modification and Analysis Laboratory (IBMAL) at the University of North Texas [10, 11]. The ion source for the ion implantation was a NEC SNICS II (source of negative ion by cesium sputtering), which is one of the three sources attached to the NEC 3 MV tandem (9SDH-2 Pelletron) accelerator. In order to avoid ion channeling effects, the samples were oriented such that there was a 7° offset from the sample surface normal and the impinging ion beams. This offset was maintained for both the H^- and Ni^- implantations. Both the H^- and Ni^- ion beams were electrostatically raster scanned through an aperture to ensure a uniform implantation circular region of approximately 1 cm in radius over the substrate. The ion beam current on the target was below the threshold for ion beam annealing

and heating effects. The Ni^- was implanted using a copper cathode filled with NiO powder mounted inside of the SNICS II source. The Ni^- ion was then selected by a mass per charge selector magnet, focused, and rastered onto the target. The Ni^- was implanted at an energy of 50 keV, with a fluence of 2×10^{15} atoms cm^{-2} . The beam current on target was approximately 20 nA. This implantation fluence was chosen so that the InP could be easily recrystallized after annealing due to lower amount of defects. The H^- implantation was performed using a copper cathode filled with TiH powder mounted inside of the SNICS II source. The resulting ion beam was put on target in the same way as the Ni beam, with a different selector magnet current. The H^- was implanted at an energy of 50 keV, with a fluence of 1.5×10^{16} atoms cm^{-2} . The H beam current on target was approximately 1.5 μA . The samples were then cut and annealed at a temperature of $450^\circ C$ for 1hr in an Ar rich environment. The as-implanted and post-annealed samples were analyzed with Rutherford Backscattering Spectrometry (RBS) and X-Ray Induced Photoelectron Spectroscopy (XPS) depth-profiling. The RBS was performed on a single ended NEC 9 SH accelerator with a 1.5 MeV He beam at the IBMAL. The samples were mounted in the RBS chamber such that it had a 0° offset from the impinging He beam and a scattering angle of 160° . The RBS spectra were analyzed using SIMNRA package [12]. The XPS was carried out using a PHI 5000 Versaprobe II Scanning XPS Microprobe with UPS at the Material Research Facility (MRF) at UNT [11]. Al monochromatic X-ray radiation (1486.6 eV) was focused to a spot size of about 200 μm . The pressure of the analysis chamber was kept initially at 5×10^{-10} mbar. In this system, the full width at half maximum (FWHM) of the Ag $3d_{5/2}$ peak was ≤ 0.50 eV for the energy range 372 eV to 365 eV. The XPS was done in conjunction with a pumped Ar ion gun to obtain a depth profile.

3. Results and Discussion

3.1 Simulation of Implant ion Distributions in InP

The implantation of the Ni and H atoms into the InP substrate were simulated using the SDTrimSP package. This ion-solid package simulates the ion range and distribution dynamically while incorporating target atom sputtering. An ion energy of 50 keV for each ion was used to ensure a large spatial distribution between the peak concentrations for Ni and H atoms. Figure 1 displays the simulated depth profile obtained for the Ni atoms implanted into InP at 50 keV with a fluence of 1.41×10^{15} atoms cm^{-2} . The simulation indicates that the peak concentration of the Ni atoms is distributed approximately 30 nm below the surface.

Figure 2 displays the simulated depth profile for 50 keV H atoms implanted into InP with a fluence of 1.06×10^{16} atoms cm^{-2} . The H peak concentration is predicted to be ~ 331 nm below the surface. Figure 3 shows the concentrations of both the Ni and H superimposed, while the implant distributions

were simulated independently. This large spatial separation was selected such that upon analysis, the accumulation of the Ni could be seen clearly when the pre and post annealed elemental profiles are compared.

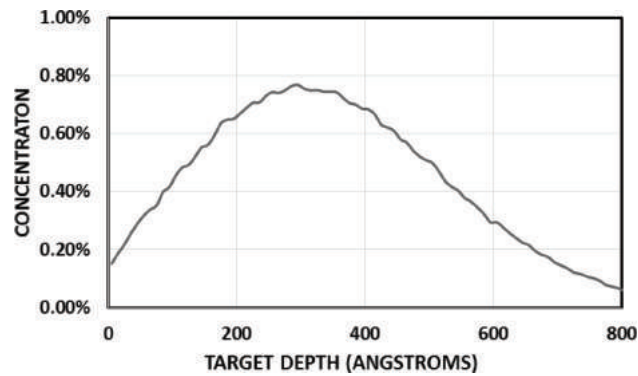


Figure 1. Simulated distribution of Ni implanted into InP at 50 keV with a fluence of 1.41×10^{15} atoms cm^{-2} .

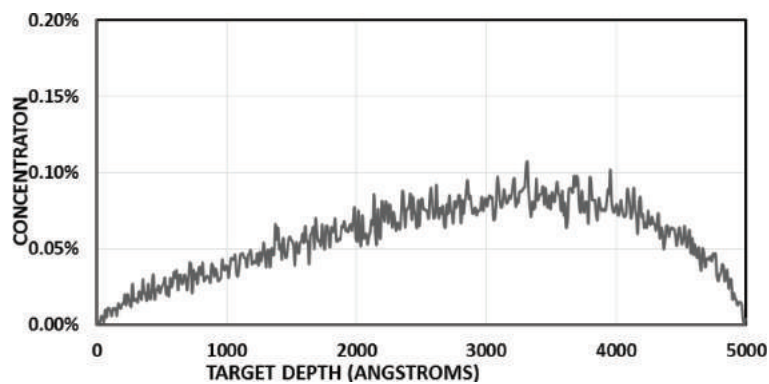


Figure 2. Simulated distribution of H, implanted into InP at 50 keV with a fluence of 1.06×10^{16} atoms cm^{-2} .

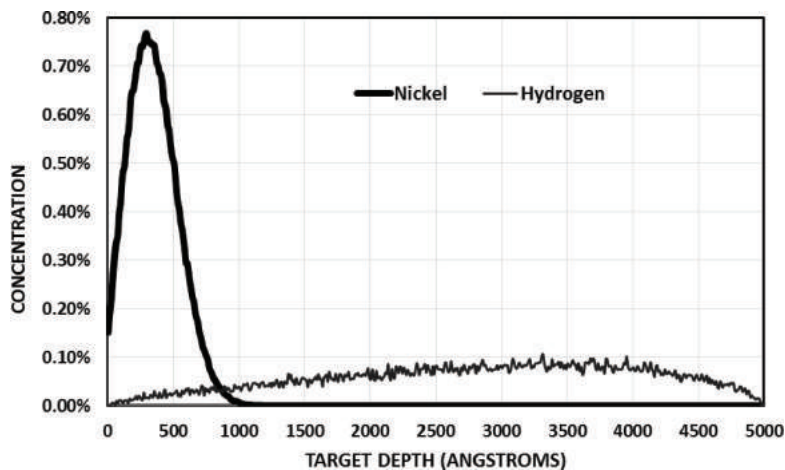


Figure 3. Simulated overlapped concentration distribution of Ni with a fluence of 1.41×10^{15} atoms cm^{-2} and H with a fluence of 1.06×10^{16} atoms cm^{-2} implanted into InP at 50 keV.

3.2 Experimental Depth Profiles of the Implanted ions using RBS and XPS Characterization Techniques

Figure 4 shows the experimental RBS spectrum and SIMNRA analysis spectrum of the 50 keV Ni as-implanted into InP sample. The SIMNRA simulated data indicated Carbon in the top 7 nm. Which may be contamination build up during the ion implantation process. Ni was seen in the layers from 7-77 nm layer peaked at a depth

of 42 nm with a peak concentration of 6%. This depth is reasonably consistent with the SDTrimSP simulation of the implantation. The RBS spectrum of the as-implantation sample also indicates that there is an accumulation of In towards the surface region by comparing the intensity of the In peak in relation to the P peak. This accumulation of In is caused primarily by the impinging Ni⁻ ions on the surface of the substrate. When the Ni⁻ ions strike the surface there is a probability of collision with either the P or In atoms. When the Ni ions collide with the P atoms this can lead

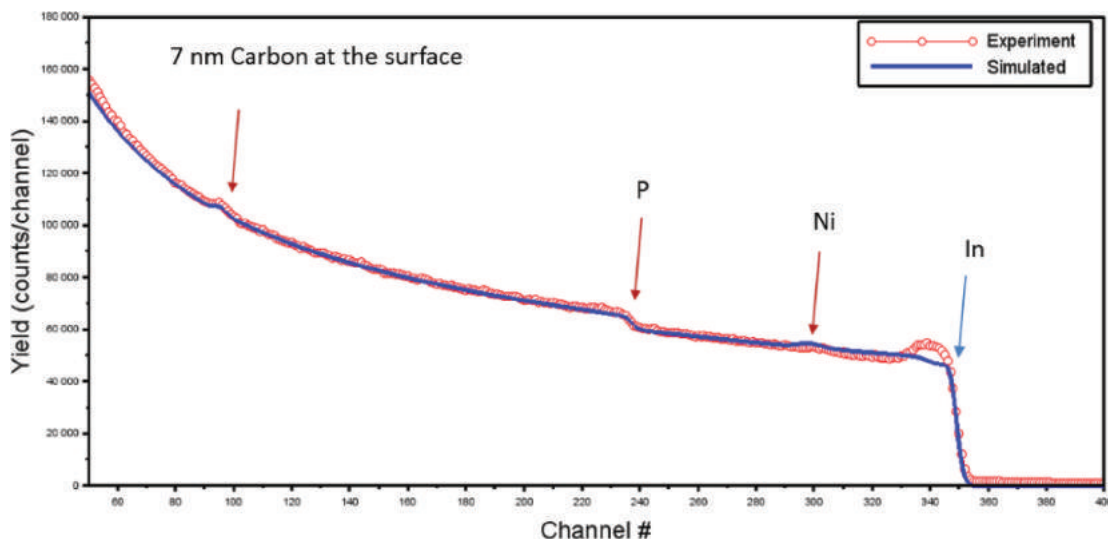


Figure 4. Experimental RBS along with SIMNRA simulated spectra of 50 keV Ni with a fluence of 2×10^{15} atoms cm^{-2} implanted into InP. A 7 nm Carbon contaminants was observed in the top layer. Ni was seen in the layers from 7-77 nm layer peaked at a depth of 42 nm with a peak concentration of 6%.

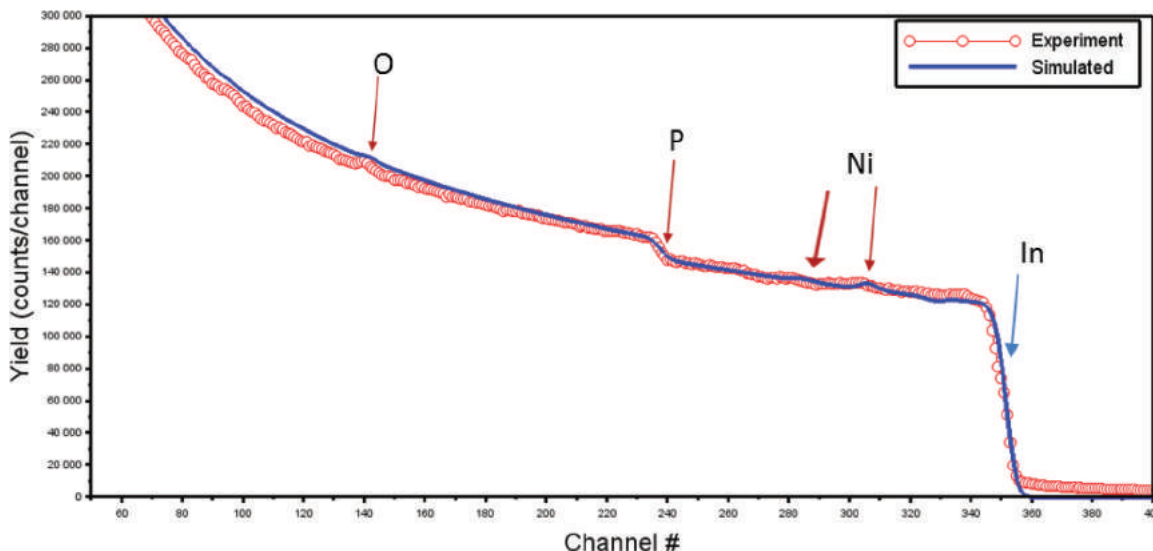


Figure 5. RBS along with SIMNRA analyzed spectra of an annealed sample. This sample was 50 keV H implanted with a fluence of 1.5×10^{16} atoms cm^{-2} into a sample which was previously implanted with Ni with a fluence of 2×10^{15} atoms cm^{-2} into InP sample. The arrows indicate the surface peak location of O, P and In. The arrows for Ni indicate the Ni signals coming from layers deeper than the surface region.

to one of two events; either the P atom is knocked out of its lattice position due to being recoiled into an interstitial position deeper in the substrate or the P is sputtered from the sample surface. Due to the mass difference between P and In, the Ni is more likely to sputter the P atoms than the In atoms, and the recoiled P atoms will have a greater depth of recoil than the In leading to the surface accumulation seen in figure 4.

Figure 5 shows the RBS along with SIMNRA analyzed spectra of an annealed sample, which was implanted with 50 keV H ions implanted into as-implanted 50 keV Ni

into InP (as shown in figure 4). The fluence of H ions was 1.5×10^{16} atoms cm^{-2} . One can see that in Figure 5, the ratio of P and In on the sample surface region has approximately returned to its pre-implanted state after annealing. The C contamination seen in the as-implanted samples appeared to be removed completely. But an additional O peak has also appeared in the post annealed data. This O peak is likely due to the oxygen contaminants in the substrate by the residual atmospheric O in the tube furnace during annealing at 450 °C for 1 hr in an Ar rich environment. The atmospheric O was given enough energy by the tube

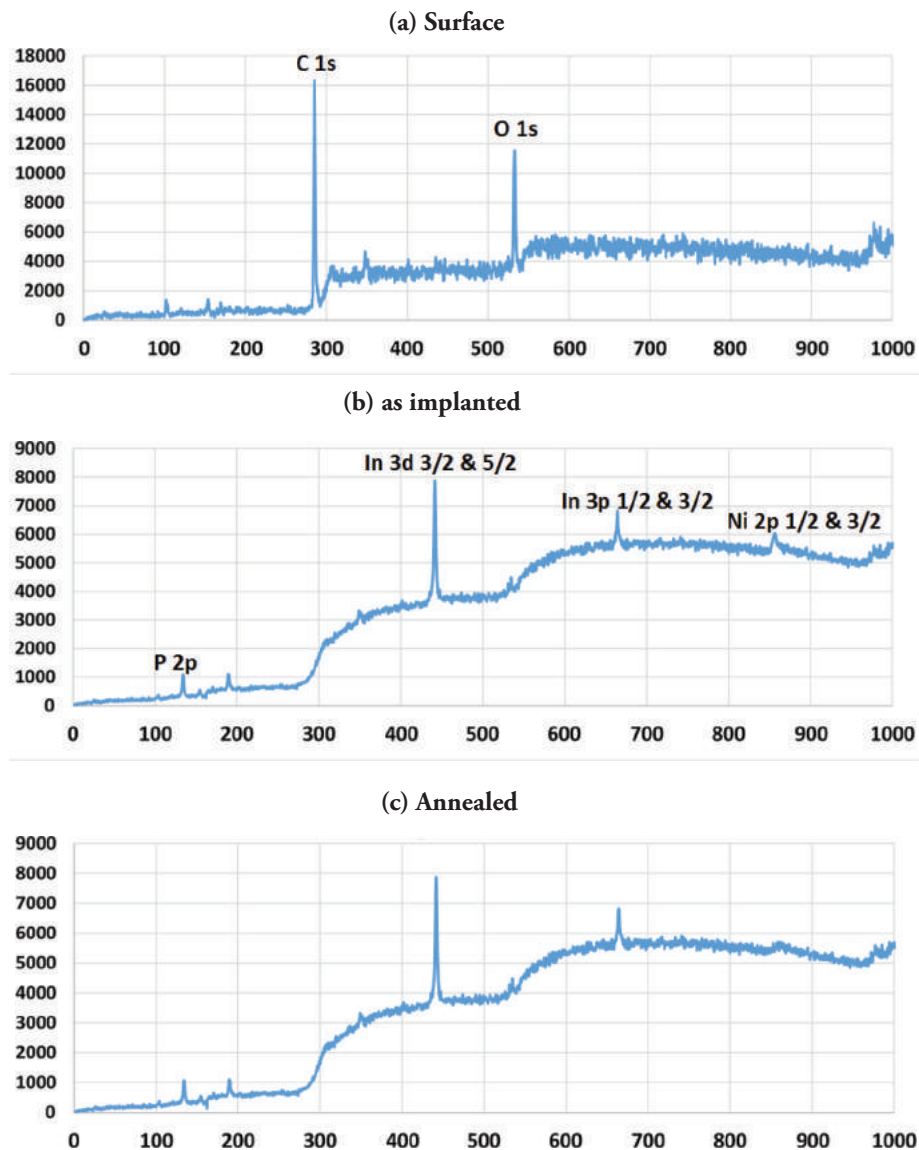


Figure 6. Typical XPS spectra of samples (a) surface of a sample with carbon and oxygen contaminants, (b) from a depth with a peak Ni concentration of as-implanted InP sample, and (c) from a depth with a peak Ni concentration of Ni and H implanted InP sample after annealing. The X-axis is the energy (eV) of the photo-electrons while the Y-axis is the counts in arbitrary units. The peaks as-shown for P, C, O, In, and Ni were used for elemental concentration profiles.

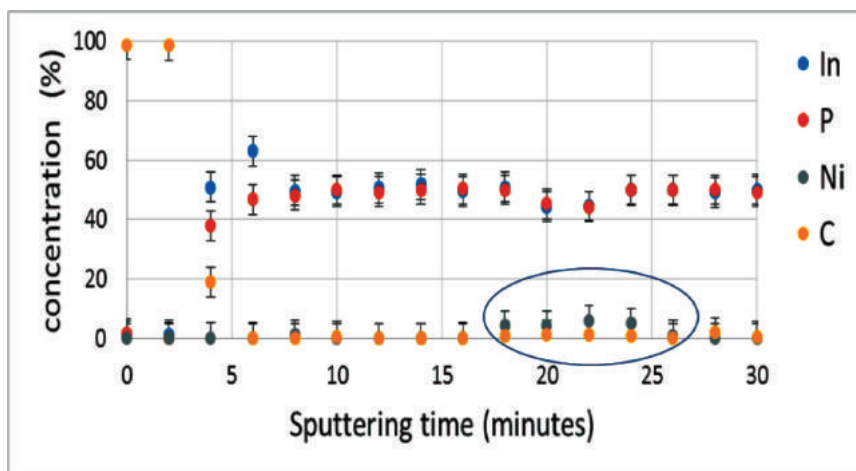


Figure 7. Elemental concentration depth profile in the as-implanted sample (50 keV Ni implanted into InP). Carbon contaminant is seen on the top surface. Ni concentrations are seen peaked between 18-24-minute sputtering cycles.

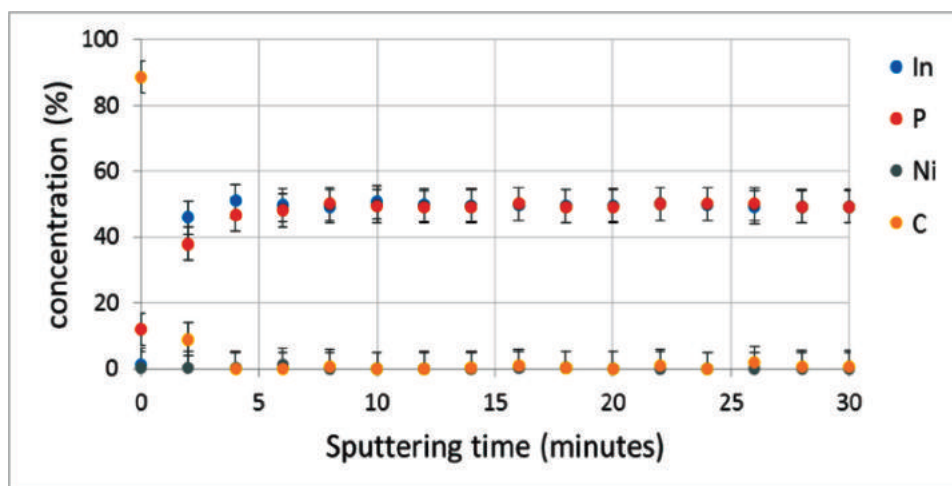


Figure 8. Elemental concentration depth profile of post-annealed sample (50 keV Ni and H implanted into InP) as extracted from XPS spectra with Ar-ion etching time/cycle. The Ni concentration was below the detection limit.

furnace to diffuse into the substrate up to 20 nm below the surface. This reasoning is believed due to the low affinity of InP to O contamination. After annealing, the top 20 nm of the substrate was determined to have a concentration of In (0.25), P (0.07), O (0.4), C (0.2), Ni (0.08) when analyzed by SIMNRA. The analysis result indicates underneath the top layer, another layer of 100 nm of InP and then further 25 nm layer of In (.485), P (.485), Ni (0.03) into the InP substrate. From the above discussion it is seen that the Ni peak (as-implanted sample) has split into two peaks after annealing, indicating that the Ni has gettered deeper into the substrate than the initial 70 nm below the surface. This gettering/accumulation of Ni atoms/clusters is probably caused by the H being outgassed during the annealing and the Ni gettering to these empty defect sites.

Figure 6 shows a typical XPS spectrum from the surfaces of 50 keV Ni and H implanted InP samples. The following peaks (P 2p (at 133.68 eV), C 1s (at 284 eV, O 1s (at 529.5 eV), In 3d (at 441.44 eV), and Ni 2p (at 855 eV) were monitored for the elemental concentration depth profile while the samples were analyzed as a function of Ar sputtering time/sequence. Appropriate background subtraction of the peaks were performed while estimating the elemental concentration ratio. Figure 7 shows the elemental concentration depth profile of the 50 keV Ni as-implanted InP samples. The concentration profiles were extracted from the corresponding XPS peaks as a function of Ar ion etching time/cycle. At the first few minutes of the sputtering (3 - 4 nm) carbon contamination is seen on the surface of the substrate which is in agreement with the RBS analysis.

Below the C contamination layer, a high concentration of In accumulation was found. Ni is seen at the 18 minutes mark peaking around 24 minutes of the sputter cycle. This corresponds to the Ni being mostly concentrated between 34.2 nm and 45.6 nm with a peak concentration at 41.8 nm which is in agreement with the RBS data. In the post annealed sample (implanted with 50 keV Ni and H into InP), figure 8 shows that the C contamination has been removed due to the annealing procedure. The In and P ratio have almost returned to their original ratio of 1:1. The concentration of Ni in the substrate after annealing is below the detection limit of the XPS detector used due to the small fluence of the implanted Ni being distributed throughout the substrate by the annealing process.

4. Conclusions

In a single ion metal implantation into semiconductors, after annealing, the metal atoms typically migrate to either to the sample surface or to the end of the initial range involving the interface of amorphous and crystalline regions of the substrate. In the 50 keV Ni implantation into InP, the initial distribution of significant amount of Ni was up to a depth of 70 nm from the surface. However, after annealing the sample (which was initially Ni implanted along with further 50 keV H ion implantation), from the RBS analysis, the Ni was found at the top 20 nm and at another region with 25 nm width at a depth of 100 nm below the top layer. The initial Ni implantation fluence was kept at a lower level for complete recovery of the substrate crystalline quality. The XPS profiling was sensitive enough to detect the Ni concentration in the as-implanted samples. However, in the annealed samples, the Ni atoms have migrated deeper with a concentration level below the detection limit of the XPS profiling. This preliminary results have demonstrated that the implanted Ni atom have indeed migrated deeper (beyond the initial end of the range) into the bulk material, most likely accumulated in defect sites left by the vacated H. In the future to improve the elemental detection sensitivity, depth-profiling experiments are planned to utilize Secondary Ion Mass Spectroscopy (SIMS).

Acknowledgements

The authors would like to thank Dr. Andreas Mutzke from the Max-Planck-Institute of Plasmaphysics, Germany, for providing the latest version of the SDTrimSP simulation code.

References

- [1] M. Zhang, X. Zeng, P. K. Chu, R. Scholz, Ch. Lin, *Journal of Vacuum Science & Technology A: Vacuum, Surfaces, and Films*. **18**, 2249 (2000).
<https://doi.org/10.1116/1.1288138>
- [2] K. Potzger, *Nuclear Instruments and Methods in Physics Research B*. **78**, 272 (2012).
- [3] R. T. Huang, C. F. Hsu, J. J. Kai, F. R. Chen, T. S. Chin, *Applied Physics Letters*. **87**, 202507 (2005).
<https://doi.org/10.1063/1.2132081>
- [4] S. Bedanta, W. Kleemann, *Journal of Physics: Applied Physics*. **42** 013001 (2009).
- [5] G. Malladi, M. Huang, T. Murray, S. Novak, A. Matsubayashi *et al. Journal of Applied Physics*. **116**, 5 (2014). <https://doi.org/10.1063/1.4892096>
- [6] M. S. Dhoubhadel, B. Rout, W. J. Lakshantha, S. K. Das, F. D'Souza *et al.*, *AIP Conference Proceedings*. **1607**, 16-23 (2014). <http://dx.doi.org/10.1063/1.4890698>.
- [7] A. Kinomura, J. S. Williams, J. Wong-Leung, M. Petravic, Nakano *et al.*, *Applied Physics Letters*. **73**, 2639 (1998). <https://doi.org/10.1063/1.122538>
- [8] B. Mohadjeri, J. S. Williams, J. Wong-Leung, *Applied Physics Letters*. **66**, 1889 (1995).
<https://doi.org/10.1063/1.113311>
- [9] A. Mutzke, R. Schneider, W. Eckstein, R. Dohmen, *MPI for Plasma Physics. SDTrimSP: Version 5.00.*, IPP Report 12/8 Garching, (2011).
- [10] B. Rout, M. S. Dhoubhadel, P. R. Poudel, V.C. Kummari, B. Pandey *et al.*, *AIP Conference Proceedings*. **1544**, 11(2013).
- [11] W. J. Lakshantha, V. C. Kummari, T. Reinert, F. D. McDaniel, B. Rout, *Nuclear Instruments and Methods*. **B 332**, 33–36 (2014).
<https://doi.org/10.1016/j.nimb.2014.02.024>
- [12] M. Mayer, *Computer simulation program of RBS, ERDA, NRA and MEIS, SIMNRA version 6.06*. The latest version is available at:
<http://home.rzg.mpg.de/~mam/>.